Polyurethane-Grafted Chitosan as New Biomaterials for Controlled Drug Delivery

ARTICLE *in* MACROMOLECULES · APRIL 2015

Impact Factor: 5.8 · DOI: 10.1021/acs.macromol.5b00030

Macromolecules

Article

pubs.acs.org/Macromolecules

Polyurethane-Grafted Chitosan as New Biomaterials for Controlled Drug Delivery

Arun Kumar Mahanta,[†] Vikas Mittal,[‡] Nitesh Singh,[§] Debabrata Dash,[§] Sudip Malik,[∥] Mohan Kumar,[⊥] and Pralay Maiti*,[†]

[†]School of Materials Science and Technology, Indian Institute of Technology (Banaras Hindu University), Varanasi 221 005, India

[‡]Department of Chemical Engineering, The Petroleum Institute, Abu Dhabi, UAE

[§]Department of Biochemistry, Institute of Medical Science, Banaras Hindu University, Varanasi 221005, India

[∥]Polymer Science Unit, Indian Association for the Cultivation of Science, Jadavpur, KolKata 700032, India

[⊥]Department of Pathology, Institute of Medical Science, Banaras Hindu University, Varanasi 221005, India

Supporting Information

ABSTRACT: The present investigation focuses on the grafting of chitosan (CHT) with diisocyanate terminated polyurethane. Solid state ^{13}C NMR spectroscopy confirms the grafting reaction and the degree of substitution (DS) was calculated from the deconvoluted area of the corresponding NMR peak. Solubility studies, swelling behavior and contact angle measurements support the hydrophobic chemical modification on CHT molecules and higher DS leads to the cross-linking of CHT molecules having polyurethane bridges resulting insolubility and regulated swelling in the graft copolymer. Molecular relaxations phenomena due to the constraint associated with the grafting have been revealed using spin−lattice relaxation tine (T_1) and shifting of peak position in tan δ curve toward lower temperature in dynamic mechanical measurement at constant frequency indicating flexible nature of graft copolymers as compared to pure CHT. The sustained drug delivery has been achieved using graft copolymers vis-à-vis pure CHT following the Fickian diffusion behavior ($n \leq 0.45$) and the release rate can be tuned by altering the DS. In depth biocompatibility studies through platelet aggregation, platelet adhesion, reactive oxygen species of the developed graft copolymers, and *in vitro* hemolysis assay and cell viability have been performed to understand its potential use in biomedical applications and compared the improved properties with respect to pure CHT. Hence, bio- and hemocompatible CHT graft copolymers have been developed with the capability of controlled and sustained drug release.

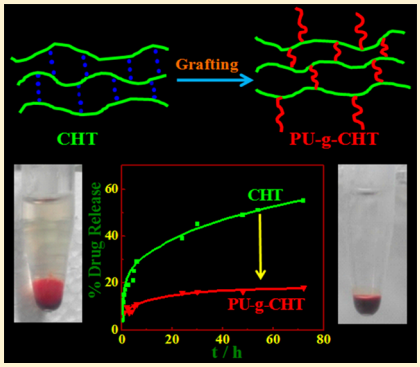

INTRODUCTION

In the last few decades, significant progress has been made on fundamental and biomedical research on chitosan technology. Chitosan is one of the most important biopolymers, composed of β-(1,4) linked 2-deoxy-2-amino-D-glucopyranose and partially of β-(1,4) linked 2-deoxy-2-acetamido-D-glucopyranose[1,2] and is obtained by alkaline deacetylation of chitin[3,4] which is the major component of the exoskeletal in crustaceans.[5] Owing to its special characteristics like nontoxic, biodegradable and biocompatible, various biomaterials of chitosan and its derivatives have been developed for its use in pharmaceuticals applications.[6−9] Chitosan can also be used in a wide range of applications such as membrane,[10] drug delivery system,[11−14] gene delivery,[15,16] cell culture,[17−19] tissue engineering,[20] biosensors,[21] and scaffold generation.[22] Although chitosan is an interesting biomacromolecule, it is insoluble in most common organic solvents and water, which greatly affects its applications in a various fields. A few chitosan derivatives have been chemically modified and characterized for their possible use in controlled release and targeted delivery of pharmaceuticals.[23,24] Some of these chitosan derivatives are self-assembled and have the capability to form nanoparticles for controlled release and targeted delivery of bioactive components. Among them, *N*-alkyl-*O*-sulfate,[25,26] cross-linked chitosan[24,25] and *O*-carboxymethylate,[24] as well as derivatives containing hydrophobic branches on chitosan backbone[25] are of great interest. *N*-Alkyl-*O*-sulfate showed nanomicelles formation and due to its self-assembly and poor solubility, slow release of paclitaxel, a hydrophobic anticancer compound, is reported in the literature.[27] Chemical modification may also improve the mucoadhesive and penetration enhancing properties of chitosan.[28] Use of chitosan derivatives for controlled release and targeted delivery of bioactive component in pharmaceutics may promote the value added use of crab and shrimp shells and enhance the growth of the seafood industry.

Now a day, the synthesis of novel blood compatible polymer-based biomaterials has been drawing great attention. Currently, much interest is being paid to use natural material for designing

Received: January 7, 2015
Revised: April 6, 2015
Published: April 17, 2015

DOI: 10.1021/acs.macromol.5b00030
Macromolecules 2015, 48, 2654−2666

new biomaterial. Very large swelling characteristics along with its fast release of drug make pure chitosan not suitable for many applications, especially in biomedical uses. Further, very low elongation at break or brittle nature of pure chitosan limits its use as biomaterials. Polyurethane-modified chitosan has become a new frontier.[29,30] Many interesting properties are expected, such as excellent mechanical property, good thermal stability, increasing anticoagulant, low hydrophilicity, and so on.

In this work, isocyanate-terminated polyurethane (prepolymer) was grafted on to chitosan molecules and various degree of substitutions with varying chain length were obtained to control the hydrophilic nature. Network structure has also been developed through cross-linking of chitosan molecules with polyurethane bridges. Grafting was confirmed by using ^{13}C solid state NMR and other spectroscopic techniques. Solubility and swelling profile of the copolymers also endorse the grafting followed by cross-linking. Thermal and mechanical properties, especially the relaxation behavior has been carried out to understand the effect of grafting. The profound effect of cage structure on drug release has been revealed to develop a sustained release system. The biocompatibility including hemo compatibility of this new class of material has been verified through MTT assay, platelet activation, hemolysis, and reactive oxygen species measurements and this novel material has been found to be suitable for tissue engineering and drug delivery. Hence, newly developed drug release systems have been designed to control the release kinetics to regulate distribution and to minimize the toxic side effects so as to enhance the therapeutic efficiency of a given drug.

EXPERIMENTAL SECTION

Materials. Chitosan (CHT), from shrimp shells with ≥75% degree of deacetylation was used for this work, was obtained from Sigma-Aldrich, USA. Poly(tetramethelene glycol) (PTMG) (Terathane, Sigma-Aldrich), number-average molecular weight (M_n) 2900 g/mol was used as received. 1, 6−hexamethylene diisocyanate (HMDI), glacial acetic acid (100%) and solvent dimethylformamide (DMF) were purchased from Merck, Germany. The catalyst dibutyltin dilaurate (DBTDL) was purchased from Himedia. The antibacterial drug, tetracycline hydrochloride was procured from Sigma-Aldrich, USA. Rhodamine B was procured from Sigma-Aldrich, USA.

Preparation of CHT-g-PU. Polyurethane-grafted chitosan copolymers were synthesized in two steps as (1) preparation of polyurethane prepolymers and (2) copolymerization through grafting.

The prepolymers were obtained through condensation reaction between HMDI and PTMG in a −NCO/−OH ratio of 1.05:1, using a few drops of 0.1 wt % DBTDL solution in toluene as catalyst. The reactions were performed at 80 °C for 2 h to form an isocyanate terminated prepolymer in a closed reaction vessel. Chitosan (1 g) was dispersed into glacial acetic acid/DMF mixture (30 mL) in the ratio of 50/50 and left overnight to obtain good swollen chitosan and consequently the grafting reaction was carried out. The isocyanate terminated polyurethane prepolymer solutions were cooled down to room temperature then fully swollen chitosan was added to the mixture. The reactions were continued at 80 °C under constant stirring for predetermined times (Table 1) to obtain various degrees of grafting/substitution. After the completion of the reaction, the reaction mixture was transferred to distilled water. Grafted copolymers were separated by filtration and successively washed with DMF, methanol, acetone to remove the pure polyurethane from grafted specimen. The final products were dried under vacuum oven at 60 °C. The reaction details are given in Scheme 1.

Characterization. *Solid State NMR Spectroscopy.* Solid-state ^{13}C NMR measurements of the samples were carried out on a Bruker 400 MHz spectrometer at the resonance frequency of 100.628 MHz using 4 mm double resonance cross-polarization magic angle spinning probe.

Table 1. Reaction Conditions and Nomenclatures of the Graft Copolymers

		time of reaction	
sample identification	degree of substitution	step 1 (h)	step 2 (min)
CHT20	20	2	10
CHT28	28	2	20
CHT34	34	2	120

Around 100 mg of sample was tightly packed into a 4 mm diameter cylindrical zirconium oxide rotor with a Kel-F end-cap. ^{13}C CP/MAS NMR spectrum was acquired with a cross-polarization contact time of 2 ms and a recycle delay of 5s at a MAS speed of 10 kHz. A 1s recycle delay was used for HP/MAS experiments in order to observe the fast relaxing components. Cross-polarization spin−lattice relaxation experiment (CPT_1) used here was a modified CP inversion recovery experiment where a single pulse delay was used between carbon pulses instead of a collection of delays. In order to observe selectively the most rigid fractions of the polymer, the single pulse delay should be about five times to that of the lowest relaxing component. A 5s single pulse delay determined from spin−lattice data of $CPXT_1$ (cross-polarization spin−lattice relaxation experiment, where, X represents heteronuclei) was used for CPT_1 experiment. All experiments were carried out at ambient probe temperature (25 °C) with high power proton decoupling during acquisition. All ^{13}C NMR spectra were assigned using adamantane as an external reference.

FTIR. Infrared spectra of the solid polymer film were recorded on a Thermo Nicolet 5700 instrument with the resolution of 4 cm^{-1} taking 100 scans at room temperature.

UV- Visible Spectroscopy. The UV−visible measurements were performed by using Shimadzu (UV-1700), pharma speck, UV−visible spectrophotometer operating in 200−1100 nm spectral range. The transparent thin films were prepared through solvent casting method.

Swelling Studies. The swelling capacity of the copolymers including CHT was determined through gravimetric technique. A known weight of the dry polymer was immersed in beaker containing 50 mL of a solution of 0.1 M AcOH and DMF mixture in the ratio of 70:30. The polymer films were taken out from the solution at different times and the excess water was removed by soaking with tissue papers. The swollen polymers were weighed and then placed in the solution again. The dynamic weight change of the polymers with respect to time was calculated using the formula below:[31]

$$\%\text{weight change} = \frac{W_f - W_i}{W_i} \times 100\%$$

where, w_f is the weight of the polymer in the swollen state and w_i is the initial weight of the polymer in dried condition.

Contact Angle. Determination of the contact angle of the graft copolymers is essential to examine their hydrophilicity. The contact angles of the copolymers were measured using the Kruss F-100 tensiometer at ambient condition. Three specimens of each sample in the form of thin strips were used to measure contact angle in water. The accuracy of the measurement was ±1°.

Differential Scanning Calorimetry (DSC). The heat of fusion of the pure CHT and its graft copolymers was determined by using DSC, Mettler 832 at a scan rate of 10° min^{-1}. The peak temperature and enthalpy of fusion were measured from the endotherms with the help of a computer attached to the instrument. The DSC was calibrated with indium before use.

The degradation temperature of the specimens was estimated using Mettler thermogravimetric analyzer at a heating rate of 20° min^{-1} under nitrogen atmosphere.

Mechanical Properties. An Instron 3369 was used to perform tensile testing at room temperature at an elongation rate of 5 mm/min. The rectangular shaped samples were used to measure mechanical properties prepared through solvent casting method. Filter paper was used to prevent the slippage of sample from the grips during

DOI: 10.1021/acs.macromol.5b00030
Macromolecules 2015, 48, 2654−2666

Scheme 1. Scheme of the Reaction Showing Time Dependent Chain Length of Grafted Species and Subsequent Cross-Linking between CHT Molecules at a Higher Degree of Substitution

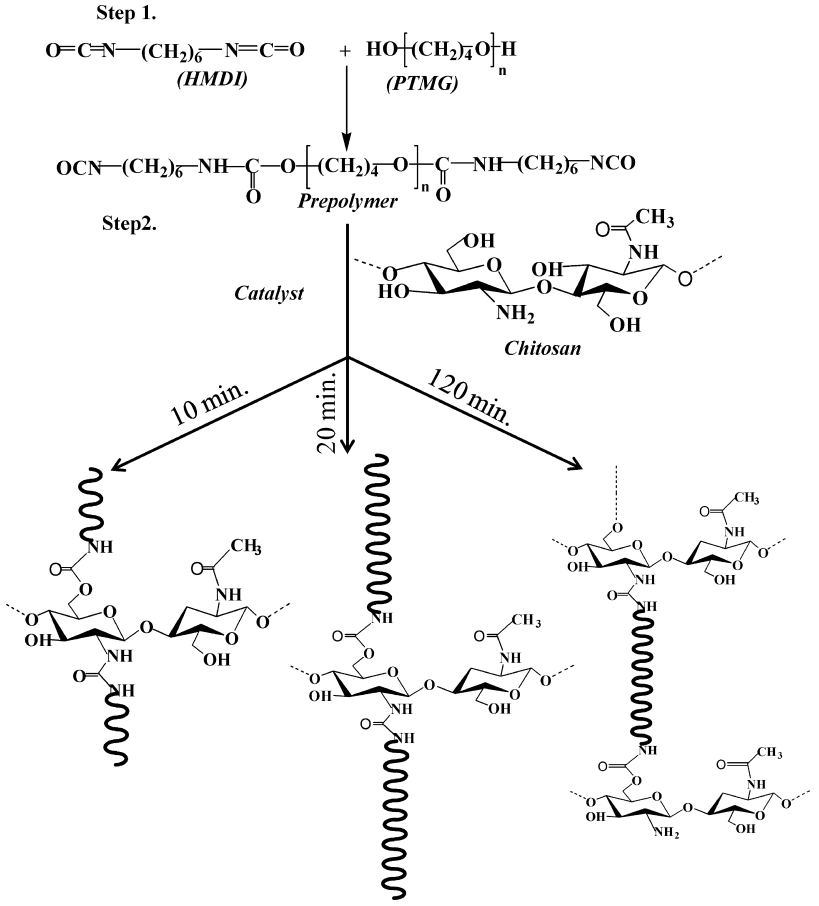

the tests. More than three specimens were tested for each sample for better error estimation.

Dynamic Mechanical Analysis. Dynamical mechanical properties of the samples were studied on thick films of pure CHT and its graft copolymers with dynamic mechanical analyzer Q 800 (TA Instruments) in the tension mode. The dynamic responses were collected from −150 to +200 °C at a constant frequency of 1 Hz with the strain amplitude of 15 μm and at a heating rate of 3 °C/min. Samples with rectangular cross section with 25 × 5 × 0.22 mm^3 dimension were used for DMA testing.

Drug Assay and Release Study. In *vitro* release studies were carried out in PBS buffer at pH ∼ 7.4. Anti bacterial drug, tetracycline hydrochloride, standard stock solution (1 mg/mL) was prepared first. The standard curve was drawn after taking absorbance using UV−visible spectrophotometer (Shimadzu 1700) taking the absorption at 358 nm in the concentration range of 1 to 10 mg/mL. CHT and its graft copolymers containing the drug were put into 100 mL of release medium in an incubator shaker (50 rpm) at 37 °C. Aliquot from drug containing solutions were taken at constant time intervals from the release medium and were replaced with same amount fresh buffer. The concentration of anti bacterial drug in the samples was measured by determining the absorbance at 358 nm.[32] Drug loaded (3 wt %) polymer film was prepared by dissolving the purified polymers and drug in a mixed solvent of 0.1 M AcOH and DMF in the ratio of 70:30. The mixture was stirred for overnight to ensure the complete dissolution of polymer and drug. The homogeneous solution of polymer and drug was poured into a Petri dish and then heated at 60 °C to evaporate solvent. After the complete evaporation of solvent, the drug embedded polymer films were used for drug release studies.

Biocompatibility. *Platelet Preparation.* Platelets were prepared from human blood following the previous publications.[33−35] In brief; peripheral venous blood was centrifuged at 180 g for 20 min in citrate phosphate dextrose adenine. The platelet rich-plasma (PRP) was incubated with acetylsalicylic acid (1 mM) for 15 min at 37 °C, which was followed by the addition of ethylene diamine tetraacetate (EDTA) (5 mM). Then, platelets were sedimented by centrifugation at 600 g for 15 min. Cells were washed using buffer A(20 mM HEPES, 138 mM NaCl. 2.9 mM KCl, 1 mM $MgCl_2$, 0.36 mM NaH_2PO_4, 1 mM ethylene glycol tetraacetic acid (EGTA), 5 mM glucose and 0.6 ADPase units of apyrase/mL, pH ∼ 6.2). Finally, cells were kept in suspended condition in buffer B (pH ∼ 7.4), which was similar to buffer A but without EGTA.

Platelet Aggregation Studies. Platelet aggregation was recorded turbidimetrically with the help of an optical lumi−aggregometer (Chrono-log model 700-2). Platelets were incubated at 37 °C for 1 min under constant stirring (1200 rpm) before the addition of polymers. Aggregation was monitored as percent of light transmitted through the samples as a function of time, while the blank represented 100% light transmittance.

In Vitro Hemolysis Study. *In vitro* hemolysis assay was carried out following the literature report.[35] In brief, human blood samples were collected from healthy volunteers. Fresh EDTA-stabilized whole blood samples were used. The red blood corpuscles (RBCs) were separated by centrifuging 1 mL blood 1:3 (v/v) with PBS at 500*g* for 10 min. The purification process was repeated for four times. Then the washed RBCs were diluted to 10 mL in PBS. To test hemolytic activity of CHT, CHT20, CHT28, and CHT34, we exposed 1 mL of RBC suspension (∼0.4 × 10^8 cells/mL) to different concentrations of CHT, CHT20, CHT28, and CHT34 in PBS. RBCs were suspended in deionized water and PBS to obtain positive and negative controls, respectively. Samples were incubated in rocking shaker at 37 °C for 4 h. Incubation was followed by centrifugation at 10000*g* for 10 min. Absorbance of hemoglobin was monitored at 540 nm, with 655 nm as a reference, in a microplate spectrophotometer (BioTek, model Power

DOI: 10.1021/acs.macromol.5b00030
Macromolecules 2015, 48, 2654−2666

Wave XS2, Medispec, India) at 37 °C. Percent hemolysis was determined using the following equation:

$$\%\text{hemolysis} = \frac{\text{sample Abs}_{540-655\text{nm}} - \text{negative control Abs}_{540-655\text{nm}}}{\text{positive control Abs}_{540-655\text{nm}} - \text{negative control Abs}_{540-655\text{nm}}} \times 100$$

MTT Assay. MTT assay determines the reduction of tetrazolium component (MTT) into an insoluble dark-purple formazan initiated by the mitochondria of viable cells. The cytotoxicity of pure polymer and its graft copolymer against platelets was determined after 2 h of exposure of platelet to different concentrations (2−100 μg/mL) of CHT, CHT20, CHT28, and CHT34. Then the samples were incubated for an additional 4 h at 37 °C with 50 μM MTT. The reduction of MTT produced insoluble formazan which was dissolved in 200 μL of DMSO and the absorbance was taken at 570 nm with the help of microplate spectrophotometer at 37 °C. In this study, positive control (100% viable) was obtained from the untreated cells.

Platelet Adhesion. Cells were charged onto slides coated either with BSA (0.1% w/v) or collagen (100 μg/mL) or pure CHT and its graft copolymers incubated for 30 min at room temperature followed by washing to observe the platelet adhesion on immobilized matrix. Cells were fixed with 4% paraformaldehyde during washing. The adhesion of cells was monitored under fluorescence microscope with phase contrast attachment (Leica model DM LB2, Lab India Instruments).

Measurement of Intracellular ROS. The oxidative activity in platelets was detected by using reactive oxygen species (ROS) sensitive probe H_2DCF-DA. The acetate groups in H_2DCF-DA are cleaved by intracellular esterase releasing the corresponding dichlorodihydrofluorescein (DCF) derivative when H_2DCF-DA diffuses into the cell. A fluorescent adduct is obtained through subsequent oxidation by intracellular ROS that is trapped inside the cell. Aliquots of platelet suspension (1×10^7 cells/mL) were incubated with 20 μM H_2DCF-DA for 20 min at 37 °C in dark. CHT and its graft copolymers (2−100 μg/mL) were added to the platelet suspension for 20 min after addition of H_2DCF-DA. The cells were then washed with PBS and the mean fluorescence intensity (MFI) was analyzed in FL1 channel of flow cytometer (FACSCalibur, BD Biosciences). Hydrogen peroxide (H_2O_2) of 10 μM was added to the platelet suspension and was taken as the positive control.

In Vivo Studies. *Rhodamine B (RhoB) Labeling of Chitosan (CHT) and Its Copolymer (CHT20).* Chitosan and its copolymer were dissolved in 0.1 M acetic acid. A predetermined amount of RhoB in water was added to those polymer solutions. The reactions were carried out for overnight at room temperature with vigorous stirring. After completion of the reaction, RhoB labeled CHT and CHT20 were obtained through the precipitation of the reaction mixture in excess acetone. RhoB labeled polymers were thoroughly washed with acetone and deionized water. Finally, the RhoB-tagged CHT and CHT20 were obtained through lyophilization.

Absorption and Tissue Distribution Assays of CHT and CHT20. The Rhodamin B labeled CHT and CHT20 were prepared in phosphate buffer saline (PBS, pH ∼ 7.4) at a concentration of 20 g/L. To determine the biodistribution of the materials, fluorescent labeled materials were orally administered to the mice through an oral gavage tube carefully passed down through the esophagus into the stomach. The feeding process using RhoB-labeled CHT and CHT20 was carried out, taking the fasting mice (12 h) of body weight ∼25 g. The total amount of solution given was 0.5 mL with a dose of 500 mg/kg. The blood samples were collected directly after a predetermined time interval and were mixed with 3 mL of 0.5 M hydrochloric acid followed by storing the suspension overnight at room temperature. The liver, kidney, heart, spleen, thymus, and lungs were collected serially after the mice were sacrificed at a predetermined time to measure the absorbed amount of materials. All the organs were homogenized using a glass homogenizer adding 3 mL of 0.5 M HCl followed by centrifugation at 2400 rpm for 20 min. Then, 3.50 mL phosphate buffer solution (PBS, pH ∼ 7.4) was added to the 0.50 mL solution of the sample. Fluorescence plate reader was used to measure the fluorescence intensity of the samples. The emission (EM) and excitation (EX) wavelength were 627 and 553 nm, respectively. Obtained fluorescence intensities were normalized with the given Rhodamine-B labeled samples. The standard curves of tagged CHT and CHT20 have been shown in the Supporting Information, Figure S1. Three mice were sacrificed for every dose of sample. The average results are presented with standard deviation (n = 3). The kidney, liver, and spleen were dissected out from mice after 4 h of administration of PBS (saline) and RhoB-CHT20 for histopathological examination. The organs were fixed by using 10 wt % formalin and then embedded into paraffin. The organs were examined using light microscopy after staining with hematoxylin−eosin (HE). The recommendations of Laboratory Animals Division, Central Drug Research Institute (Lucknow, India) and the Laboratory Animal Welfare Committee of the Institute of Medical Sciences, Banaras Hindu University were followed to carry out the animal studies.

RESULTS AND DISCUSSION

Grafting on Chitosan. Polyurethane chain extension on chitosan backbone has been done through the reaction of isocyanate terminated polyurethane prepolymer and hydroxyl/amine linkages present in chitosan. ^{13}C solid state NMR spectroscopic technique has been used to characterize the grafting and to measure the degree of substitution. Figure 1

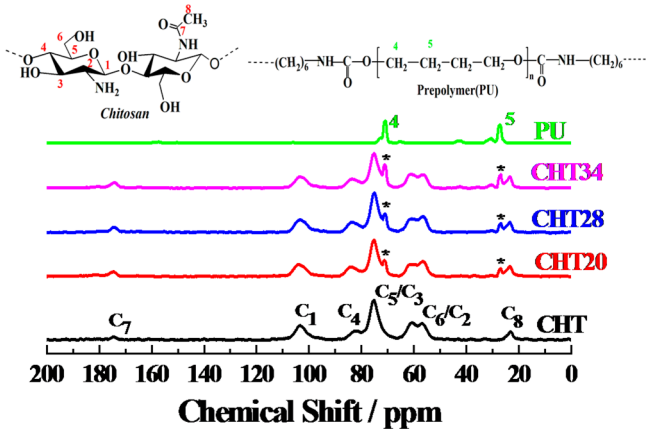

Figure 1. ^{13}C solid state NMR spectra of chitosan, PU, and their graft copolymers as indicated.

shows the ^{13}C NMR of prepolymer PU, pristine CHT, and their graft copolymers, and the assignment of each peak has been made on the basis of literature reports.[36−38] The grafting of polyurethane onto chitosan occurred through the formation of urethane (−OCONH−) linkage, with either the reaction between $-NH_2$ groups at C_2 and/or −OH groups at C_6 position of the chitosan with the −NCO terminal groups of polyurethane prepolymers resulting no change in characteristic ^{13}C NMR peak of chitosan; instead, two new peaks are observed at 26.9 and 71 ppm, respectively, in the copolymers. Moreover, the intensities of those peaks gradually enhanced with increasing the time of reaction between prepolymer (PU) and pristine CHT indicate greater incorporation of PU chain in CHT backbone at longer reaction time. The degree of substitution (DS) has been calculated from the peak area of the deconvoluted peaks and, henceforth, termed the copolymers as CHT20, CHT28 and CHT34, where the numbers after CHT represent the percentage substitution (Table 1). Degree

DOI: 10.1021/acs.macromol.5b00030
Macromolecules 2015, 48, 2654−2666

Table 2. ^{13}C Spin−Lattice Relaxation Time (T_1, s) for Chitosan and Its Graft Copolymers for Indicated Carbon Positions

CHT	CHT10	CHT20	CHT34
10.1 (C_2), 0.84 (C_6)	11.8 (C_2), 0.92 (C_6)	13.4 (C_2), 1.1 (C_6)	13.6 (C_2), 1.4 (C_6)

of substitution per chitosan monomeric unit was estimated from NMR data using the following equation:

$$\mathrm{DS}\% = \frac{\text{area of } I_{26.9\mathrm{ppm}}}{\text{area of } I_{26.9\mathrm{ppm}} + \text{area of } I_{23.35\mathrm{ppm}}} \times 100 \quad (1)$$

This is to be noted that DS increases with reaction time as newer sites are grafted and longer PU chains are attached with CHT molecules resulting cross-linking between CHT molecules through PU chain as described in Scheme 1. However, varying length of grafted PU chain has been prepared by changing the reaction time/degree of substitution which lead to the ultimate cross-linking of CHT molecules through PU chains, thereby modifying the chemical nature of CHT from hydrophilic to hydrophobic in nature. As there are three different sites from where chain extension of PU may start, it is important to find out the exact locations of chain reaction. Spin−lattice relaxation time (T_1) has been measured using inversion recovery experiments to understand the dynamics of various carbon atoms of CHT.[39] Relaxation time of C_2 and C_6 nuclei are considerably affected with degree of substitution (Table 2). T_1 increases systematically with DS both for C_2 and C_6 nuclei indicating slower dynamics arising from longer PU chains attached or actual reaction sites of chain propagation (Supporting Information, Scheme S1). Relaxation behavior as a function of time has been shown in the Supporting Information, Figure S2, exhibiting a relaxation peak at higher time. However, it is clear from spin−lattice relaxation time (T_1) that rigidity occurs in C_2 and C_6 nuclei with increase in reaction time as compared to other site and suggests the chain extension at those sites leading to ultimate cross-linking shown in the Supporting Information, Schemes S1 and S2.

Polyurethane grafting on CHT has been analyzed through spectroscopic techniques. FTIR spectra of chitosan and its graft copolymers CHT20, CHT28, and CHT34 are shown in Figure 2. The well-known characteristics peaks of chitosan are shown (Supporting Information, Figure S3) at 1650 and 1580 cm^{-1} for distinct amide I and amide II bands, respectively.[40] The broad peaks in the region of 3200−3500 cm^{-1} were assigned for N−H and O−H stretching vibration of inter- and intramolecular hydrogen bonds appears from the $-NH_2$ and

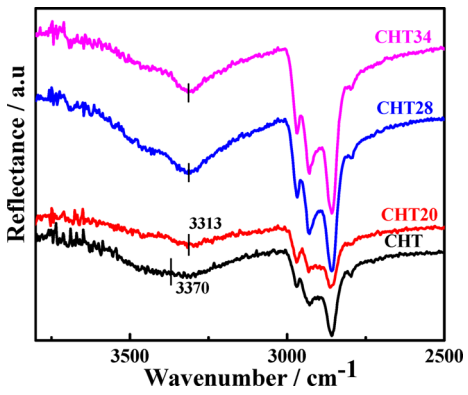

Figure 2. FTIR spectra of CHT and its indicated copolymers. The vertical lines indicate the peak positions.

−OH groups of the chitosan molecule.[40,41] Observed band of pure CHT at 3370 cm^{-1} becomes narrower as well as shifted to lower region at 3313 cm^{-1} in graft copolymers with increasing the degree of substitution suggest that the inter- and intramolecular hydrogen bonding become weak as the $-NH_2$ and −OH groups of CHT have been transformed into corresponding urea and urethane linkages. The shifting of the band is attributed to the interaction between grafted PU and CHT molecules mainly due to dipolar interaction including hydrogen bonding. The UV−Vis spectra of polyurethane, pure chitosan and its graft copolymers are shown in Figure 3.

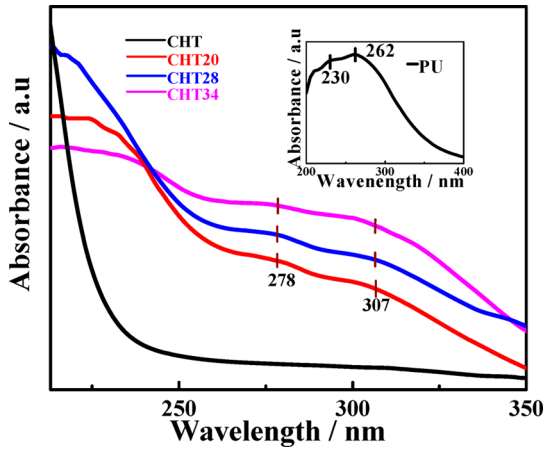

Figure 3. UV−visible spectra of CHT and its indicated copolymers. The vertical lines indicate the peak positions. Inset figure represents the UV−vis pattern of pure PU showing absorption peaks.

Pristine CHT shows no absorption peak in the range of 200−400 nm[42] while PU shows one band at 230 and 318 nm due to the $\pi-\pi^*$ and $n-\pi^*$ transition, respectively.[43] Notably, the UV−vis absorption peaks of grafted copolymer are shifted to longer wavelengths at 278 and 307 nm. The red shifts are attributed to the interaction between PU and CHT chains. These results are consistent with the literature reported value of grafted chitosan.[42,44]

Effect of Grafting. Grafting plays an important role for modifying the properties and makes the polymer suitable for different applications. CHT is soluble in dilute mineral acid while PU is soluble in DMF. The solubility of the copolymers has been carried out in 0.1 M acetic acid and in acetic acid/DMF mixture in the ratio of 70/30. The grafted copolymer CHT20 is soluble in both acetic acid and acetic acid/DMF mixture, whereas CHT28 is partially soluble in 0.1 M acetic acid but soluble in acetic acid/DMF mixture. On the contrary, CHT34 is insoluble in both the solvents. It is evident from the solubility studies that slightly longer grafting of PU chain makes CHT partially soluble in acetic acid solution while cross-linking of CHT at longer reaction time (CHT34) convert into insoluble system.

Swelling studies provide important indication of the extent of cross-linking in a polymer network.[45] Figure 4 exhibits the swelling behavior of graft copolymers indicating poor swelling for higher DS copolymers. The swelling decreases considerably

DOI: 10.1021/acs.macromol.5b00030
Macromolecules 2015, 48, 2654−2666

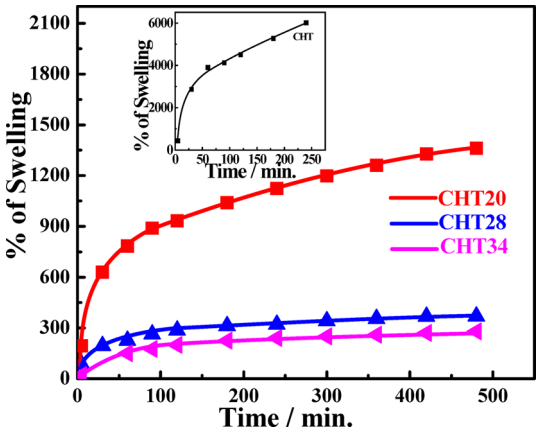

Figure 4. Swelling profile of chitosan (inset figure) and its indicated graft copolymers in acetic acid and DMF mixture.

with increase in cross-link densities. Swelling behavior of pure CHT has been presented in the inset of Figure 4 showing very high swelling (6000%) of pure CHT and it can be tuned nicely up to 200% by controlling the DS or cross-link density through grafting. Grafting of CHT with polyurethane transforms the polymer toward hydrophobic in nature as evident from the higher contact angle of copolymers as compared to pure CHT (Supporting Information, Figure S4). Further, the contact angle enhances with DS indicating wrapping up of hydrophobic PU on CHT molecules. However, the degree of swelling systematically decreases to 1360, 370, and 280% for CHT20, CHT28 and CHT34, respectively, while increase of contact angle is noticed as 66.6, 70.7, and 72.2° for the same order of specimens. However, the solubility, swelling ability, and contact angle of grafted and cross-linked chitosan have particular importance as a drug carrier.

Effect of Grafting on Thermal and Mechanical Responses. Thermal degradation profiles for pristine and chemically modified chitosan are quite different. The mass losses curves, evaluated under nitrogen atmosphere, are shown in Figure 5a. Pure polymers exhibit single step degradation while graft copolymers show two steps degradations corresponding to the copolymer components. The initial mass loss, occurred at 45 °C which continued up to 150 °C with gradual weight loss of 5%, is associated with the loss of adsorbed water molecules due to hydrophilic nature of polymer. The second stage of degradation started at 281 °C with 50% weight loss corresponding to the decomposition of chitosan.[47,48] The third stage of weight loss in graft copolymers corresponds to the PU degradation at ~400 °C. The thermogravimetric analysis was used to determine the thermal stability of chitosan where it is expected to decrease its weight with increasing cross-linking due to disappearance of hydrogen bonding associated with *N*-acetyl and free amino groups in graft copolymers.[46] Pure prepolymer (PU) shows single stage degradation which starts at higher temperature (395 °C) as compared to chitosan and nearly complete degradation occurs at 450 °C. On the other hand, around 60% degradation occurs for CHT due to formation carbon shoot which get enhanced considerably in graft copolymer.

DSC curves of chitosan and its graft copolymers under nitrogen atmosphere are shown in Figure 5b. A broad endothermic peak around 50 °C is observed in the DSC curve of chitosan which is attributed to the loss of absorbed water and another strong exothermic peak centered near 307 °C due to the decomposition of chitosan which is in good agreement with the TGA analysis.[49,50] Prepolymer (PU) shows a sharp endotherm at 48.1 °C indicating its melting point while the graft copolymers show endothermic peak at ~40 °C. The lowering of melting temperature is presumably due to the dilution effect and greater interaction between PU and CHT chains. The interactions are further reflected in reduced heat of fusion (ΔH) of copolymers as compared to pure PU. ΔH gradually decrease with increasing DS due to reduction in crystalline part after cross-linking.[48] However, chitosan does not show any characteristics glass transition temperature (T_g) in its DSC curve. It is well-known that chitosan is a semicrystalline polymer and shows strong intra- and intermolecular hydrogen bonding along with a rigid amorphous phase of its heterocyclic units. The variation in heat capacity corresponding to the change in specific volume near T_g is too small to be detected by using DSC. A more sensitive method by applying sine wave frequency (DMA measurement) has been used to detect the T_g.

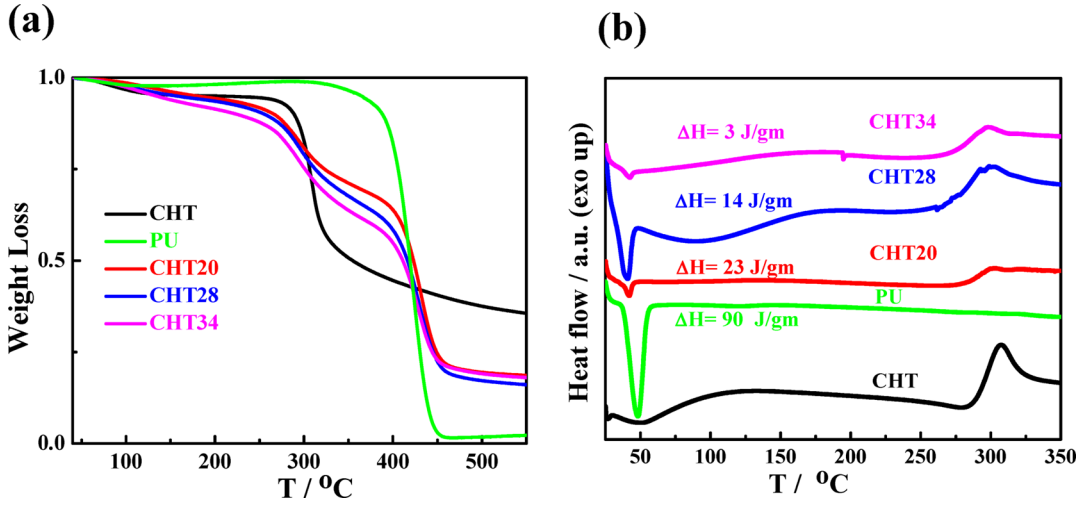

Figure 5. (a) TGA and (b) DSC thermograms of CHT and its graft copolymers. The heat of fusion gradually decreases with increasing DS as mentioned.

DOI: 10.1021/acs.macromol.5b00030
Macromolecules 2015, 48, 2654−2666

Dynamic mechanical analysis is a sensitive probe to investigate the relaxation process associated with the molecular motion in a polymer.[51] Figure 6 shows the dynamic mechanical

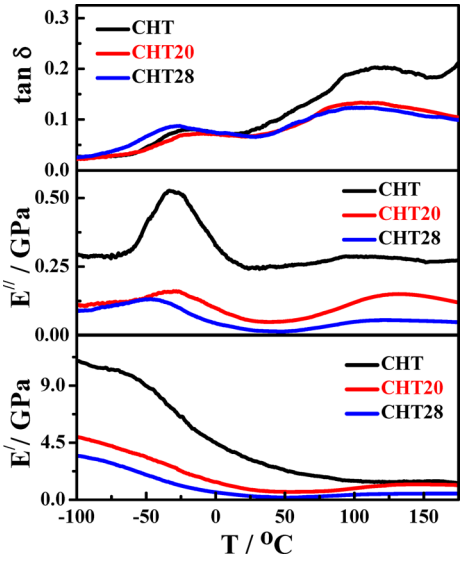

Figure 6. Dynamic mechanical responses of pure CHT and its graft copolymers as a function of temperature in tensile mode, tan δ curves (top), loss modulus (middle) and storage modulus (bottom).

behavior of CHT and its graft copolymers in the temperature range of −150 to +200 °C measured at a frequency of 1 Hz. Pristine CHT film shows two relaxations at −20 °C, β relaxation characteristic of the local motion of side chain groups in chitosan molecule, and at 118 °C, α-relaxation or glass transition temperature (T_g). Mucha et al. considered the β relaxation as typical water relaxation,[52] consequently, the decrease of this temperature for graft copolymer (−30 °C) is due to disappearance of hydrogen bond arising from the grafting reaction in −OH or $-NH_2$ linkages of CHT. The glass transition temperature for the copolymers decreases to 104 and 102 °C for CHT20 and CHT28, respectively. The decrease in glass transition temperature is associated with the degree of substitution, as greater degree of substitution decrease the amount of free −OH and $-NH_2$ groups in chitosan matrix resulting weaker inter- and intrahydrogen bond formation among molecules. A very broad temperature, ranging from −23 to 203 °C, is reported in the literature[49,53,54] as the T_g of chitosan. The storage modulus (E') also simultaneously decreases with increasing the degree of substitution in graft copolymer and exhibits values of 10.4, 4.6, and 3.2 GPa for CHT, CHT20, and CHT28, respectively, for a similar reason. This is to mention that the measurement of CHT34 was not possible because of its brittle nature arising from highly cross-linked behavior as discussed earlier. Loss modulus of the graft copolymers substantially decreases as compared to pure CHT, due to increased rigidity emerging from the grafting of PU on CHT backbone.

Figure 7 represents the stress−strain curves of CHT and its copolymers under uniaxial tension. Young's modulus decreases significantly for graft copolymers in comparison to pure CHT (Table 3), similar trends obtained in DMA measurements. Extensive hydrogen bonding in CHT makes it a rigid system which exhibits high modulus. On the contrary, grafting in −OH and $-NH_2$ groups transform the graft copolymers less

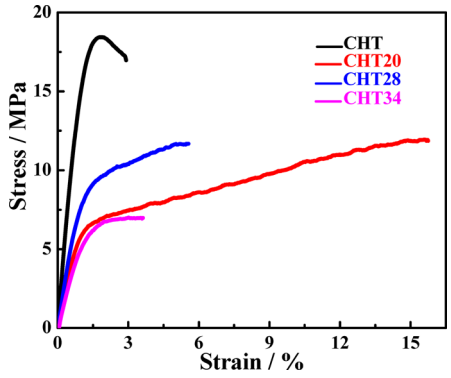

Figure 7. Stress−strain curves for pure CHT and its graft copolymers.

Table 3. Mechanical Properties of Pure CHT and Various Graft Copolymers under Uniaxial Tension

sample	modulus (MPa)	toughness (MJ/m^3)	elongation of break (%)	ultimate strength (MPa)
CHT	18.78	42.18	2.93	18.46
CHT20	7.24	143.15	15.76	11.84
CHT28	9.21	52.51	5.59	11.67
CHT34	5.28	20.83	3.62	6.97

hydrophilic and the possibility of forming hydrogen bond is drastically reduced causing a flexible system in the graft copolymers. The percentage elongation at break substantially increases in graft copolymers with a general trend of decreasing elongation at break for greater DS. Moreover, the toughness, measured area under the stress−strain curve, increases for graft copolymer vis-à-vis pristine CHT, except for CHT34 which is a highly cross-linked system (Table 3). Thus, both steady state and dynamic measurements of mechanical properties clearly demonstrate that the flexibility of CHT molecules enhances along with the three-dimensional network in graft copolymer with increasing the degree of substitution. Therefore, graft copolymers have potential for its use as drug carrier for controlled release with their added flexibility and network structure.

Controlled Release of Drug. The aim of a controlled drug delivery system is to supply a biologically active molecule depend on the need of the physiological environment over a required time period maintaining the drug level in the body within the therapeutic window. *In vitro* drug release kinetics were performed in phosphate buffer solution (pH ∼ 7.4) at 37 °C using tetracycline hydrochloride loaded biocompatible and hemocompatible pristine CHT and polyurethane grafted chitosan films. Figure 8 shows the cumulative percentage release of tetracycline hydrochloride as a function of immersion time. The sustained release of drug from PU grafted CHT copolymers is obvious vis-à-vis pure CHT. Pure CHT exhibits fast release of drug and release rate remains high at longer period and the total drug release attains 60% in 72 h. On the other hand, gradually sustained release has been noticed in graft copolymers with higher degree of substitution (only 15% release for CHT34 in 72 h). Moreover, the burst release completely disappears in graft copolymers, and the cumulative releases are 60, 30, 20, and 15% for pure CHT, CHT20, CHT28, and CHT34, respectively, during the first 72 h. Even though the absolute value of drug release is low in case of graft copolymer, it gradually releases with increasing time as is evident in the case of CHT34. A comparative measurement

DOI: 10.1021/acs.macromol.5b00030
Macromolecules 2015, 48, 2654−2666

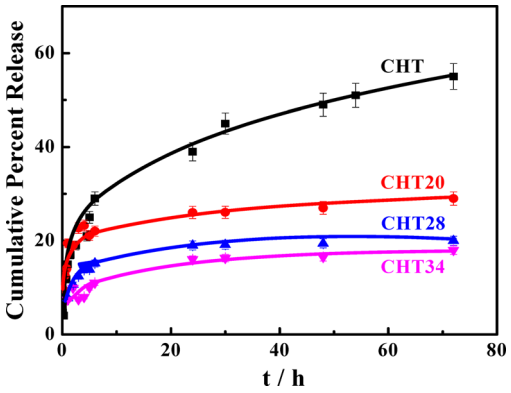

Figure 8. Cumulative drug release profile for CHT and its indicated graft copolymers. The solid lines are the guide to the eye.

shows that 18% of drug release occurs in time 0.8, 2, 18, and 72 h in pure CHT, CHT20, CHT28, and CHT34, respectively, exhibiting sustained release in highly graft copolymer as compared to pure CHT. If we look into the mechanism of drug release from a polymer matrix, liquid penetration into the matrix, dissolution of the drug and diffusion of drug out of the matrix are the three distinct steps.[61] The rate-determining step for drug release may be any one of these processes. It is observed that the release of drug molecules is significantly delayed from the graft copolymers than the pristine CHT. Polyurethane grafted chitosan systems show greater extent of network structure through cross-linking with increase in degree of substitution on to chitosan backbone. Increased cross-linking produces denser network and exhibits restricted swelling due to larger retraction forces caused by the higher number of covalent bridges within in the system and simultaneously prevents the diffusion out of the drug molecules from the network to the release medium. The release kinetics of tetracycline hydrochloride from PU grafted CHT copolymers are best fitted with the Korsmeyer–Peppas model leading to the exponent "n" values of 0.27, 0.11, 0.13, and 0.21 for CHT, CHT20, CHT28, and CHT34, respectively, indicating the Fickian ($n < 0.45$) nature of drug diffusion from CHT and its graft copolymers (Supporting Information, Figure S5 and Table S1). Zero order, first order and Higuchi models are also verified but the correlation coefficient (r^2) values corresponding to those models are not satisfactory while the Korsmeyer–Peppas model is a perfect fit. Hence, slower diffusion is considered to be the rate-determining step which is strongly influenced by the sluggish swelling ability of grafted copolymer as compared to pure CHT. On the basis of the release rate, a model has been proposed in Scheme 2 to reveal the controlled release of drug from pure and graft copolymer. Extra covalent bonds arising from the extensive grafting form the network structure and diffusion of drug becomes slower from the graft copolymer cage. In summary, the drug release rate can be tuned by changing the network structure via suitable grafting of CHT.

Grafted Chitosan as Biomaterial. Materials injected intravenously for biomedical applications, like biosensor, implant, cell imaging, and drug delivery, are bound to encounter and possibly interact with blood cells, in particular, platelets and red blood cells (RBCs), much before the materials reach the target tissue. Platelets are highly sensitive than RBCs which are inert carrier of oxygen and react to minor changes in environmental stimuli leading to platelet aggregation and adhesion. Platelet aggregation and adhesion have important

Scheme 2. Drug Release from Pure Polymer and Its Grafted Copolymer Showing Faster Release in Pure CHT against Sustained Release from Network Structure in Graft Copolymer

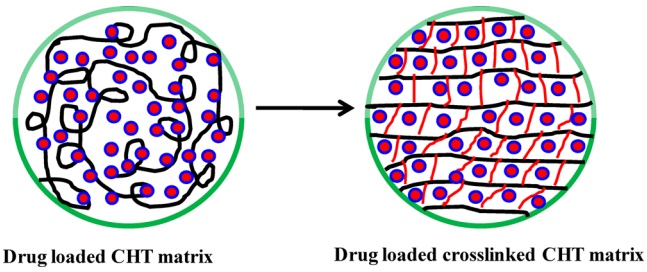

roles in thrombus formation. Such a type of platelet activation would lead to acute myocardial infarction, stroke, and arterial blockage. Interaction of platelets with the surface of the biomaterial is an important factor for the determination of the hemocompatibility of the materials.[56−60] Recently, it has been found that materials can potentially induce integrin-mediated platelet aggregation, both in vitro and in vivo, on a scale comparable to that obtained by thrombin, one of the most potent physiological agonists of platelets.[54−58] In keeping with this observation, the effect of graft copolymers on platelet function has been studied to determine the efficacy of the modification on CHT. Platelet aggregation occurs heavily upon the addition of thrombin, a known agonist, to a suspension of freshly isolated human platelets triggered by a strong wave of cell aggregation (amplitude 80%) as shown in the tracing 4 of Figure 9a. However, pure CHT (up to 5 μg/mL concentration)

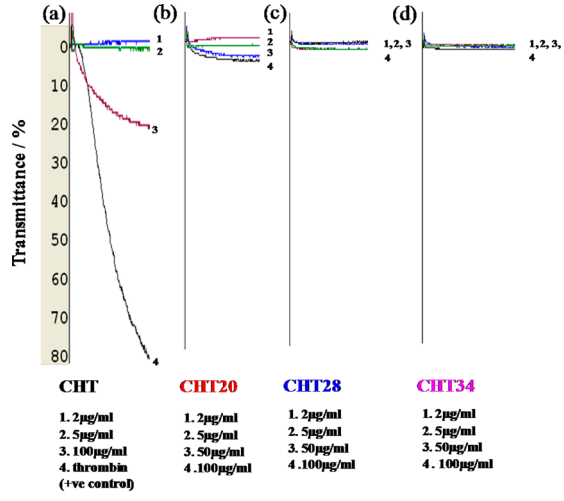

Figure 9. Effect of differentially modified polymers of CHT and its graft copolymer on platelet function. Platelet aggregation was induced by different concentration of reagents as indicated. Thrombin was used as a control.

does not induce platelet aggregation (tracing 1 and 2) while the CHT concentration of 100 μg/mL exhibits significant aggregation (trace 3 of Figure 9a with the amplitude of 20%). Interestingly, the graft copolymers CHT20 and CHT28 show very little aggregation (amplitude <5%) and CHT34 does not induce any platelet aggregation even at higher concentrations of 100 μg/mL (Figure 9b–d). Hence, platelet aggregation is completely suppressed by grafting of CHT with PU, and cross-linked CHT is found to be best hemocompatible material.

DOI: 10.1021/acs.macromol.5b00030
Macromolecules 2015, 48, 2654–2666

Platelets do adhere to the exposed subendothelial surface through interaction with collagen and von Willebrand factor.[60] The shape of the platelets became changed, allowing more contacts between the platelet surfaces and tissue for better adhesion. In this context, the adhesion of platelets on differentially grafted copolymer has been studied (Figure 10).

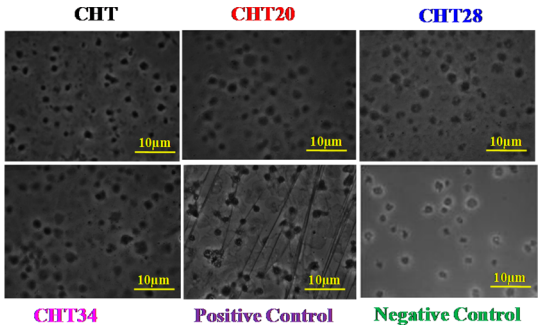

Figure 10. Adhesion and spreading of platelets on immobilized matrices BSA, collagen, on pure CHT and its indicated graft copolymers. The collagen fiber was used to perform positive control.

Platelets undergo shape change or spreading on adhesion to collagen matrix as expected, which have been shown in positive control. However, pure CHT and its graft copolymers do not show any change in platelet shape, which are more or less similar to the negative control with BSA. The platelet adhesion study is consistent with minimal platelet activation. Hence, graft copolymers (CHT20, CHT28, and CHT34) exhibit high hemocompatibility and show better results than that of pure CHT and do not alter the biology of circulating blood cells and maintain the platelets in a resting state.

Erythrocyte Membrane Integrity and Cytotoxicity of Graft Copolymer. Red blood cells (RBCs) are the most abundant cell in blood. RBCs come in contact with the materials surface whenever any material is inserted/injected into the bloodstream. If the material is incompatible with blood, the erythrocyte cell membrane gets rupture releasing their cytoplasm in the surrounding and spread the red color across the solution. Similar concentrations of CHT and its graft copolymers were used to study the effect of erythrocyte membrane integrity as reported in Figure 11. Pure CHT does not exhibit any hemolytic activity up to a moderate concentration of 5 μg/mL but at higher concentrations (50 and 100 μg/mL) the surface membrane got rupture and release free hemoglobin in the medium causing hemolysis. Graft copolymers (CHT20 and CHT28) show insignificant hemolysis at higher concentration while CHT34 does not exhibit any hemolysis even at higher concentration (100 μg/mL). Percent hemolysis of all the specimens at various concentrations have been provided in the Supporting Information, Table S2.

Cytotoxicity through MTT assay has been performed to confirm the biocompatibility of CHT and its graft copolymers. MTT is known as the reduction of tetrazolium dye MTT to formazan in viable cells by mitochondrial reductase, exhibiting purple color. Formazan production was measured after 2 h of exposure of different concentrations (2−100 μg/mL) of specimens against a control of platelets without any polymers. It is clearly observed from Figure 12 that pristine CHT and its copolymers at low concentration give similar viability as that of control i.e. no cell death occurred while at higher concentration cell viability reduces for pure CHT. Interestingly, the cell

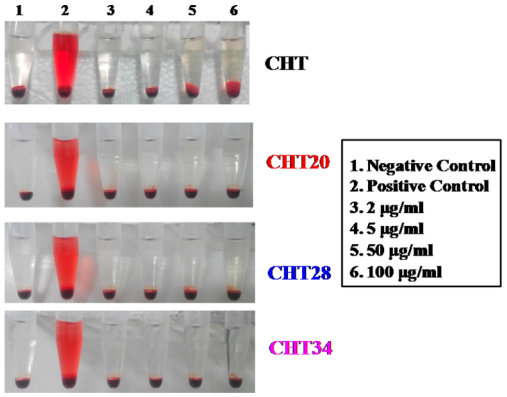

Figure 11. Effect of differentially functionalized polymers as indicated on erythrocyte membrane integrity. RBC suspensions were exposed to varying concentration (2, 5, 50, and 100 μg/mL) of CHT, CHT20, CHT28, and CHT34 for 4 h followed by centrifugation. Positive and negative controls represent RBCs suspended in deionized water and RBCs suspended in phosphate buffer saline. Images of positive and negative controls are same for each experiment.

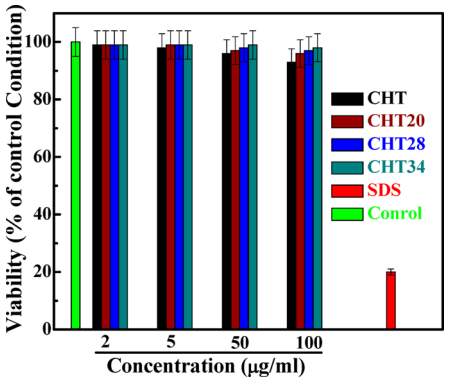

Figure 12. MTT assay of different copolymers-treated platelets. Mean values are reported from three independent experiments and are presented with standard deviation. SDS was used as a positive control.

viability increases with greater DS at higher concentrations (50−100 μg/mL) and, thereby, confirm the better biocompatibility of graft copolymer vis-à-vis pure CHT. SDS (1 wt %) treated platelet was taken as the positive control. However, MTT assay and hemolysis studies indicate nontoxic and better biocompatible nature of graft copolymers than that of pure CHT and the overall biocompatibility increases with degree of substitution in graft copolymer.

Reactive oxygen species (ROS) are chemically reactive molecules containing oxygen which have important roles in cell signaling and homeostasis. Increment in ROS level may result in significant damage in cell structures. Such type of free radicals can adversely alter protein, lipid, and DNA and have been connected with aging and a number of human diseases.[62,63] We studied whether pristine CHT and copolymers could elicit generation of ROS in platelets. H_2DCF/DA (20 μM)-loaded platelets were exposed to different concentrations of specimens at 37 °C for 10 min, and the changes in MFI were monitored through flow cytometer (Figure 13). The results showed that both CHT and graft copolymers exhibit ROS level as that of control at low concentration while ROS level gradually increases with increasing concentration for pure CHT. On the contrary, ROS levels remain low for graft copolymers even at higher concentration. Further, ROS level

DOI: 10.1021/acs.macromol.5b00030
Macromolecules 2015, 48, 2654−2666

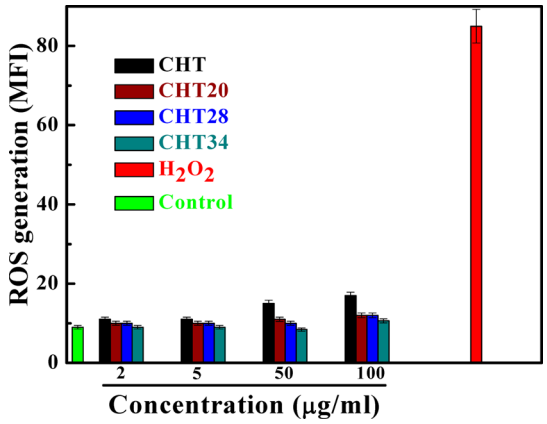

Figure 13. ROS generation in H_2DCF-loaded platelets treated with different concentrations of CHT, CHT20, CHT28, and CHT34 as indicated in the bar diagram.

gradually decrease with increasing DS of graft copolymer and exhibit lowest value in case of cross-linked copolymer (CHT34). This is to mention that 10 μM H_2O_2 was used as a positive control which displays very high ROS level due to the generation of hydroxyl free radical.

Absorption of Graft Copolymer in Blood. The concentration of materials in blood reflects the intestinal absorption of the materials.[64] The concentration of material in plasma was calculated from fluorescence intensity as a function of circulation time and has been shown in Figure 14a. It is evident that the concentration of CHT20 is considerably lower than the CHT concentration in plasma for the whole range of time. Initially, the concentration increases up to 1 h of circulation time followed by the steady decrease in concentration both for CHT and CHT20 as the materials excreted out from the blood during course of time. Absorption and distribution of chitosan is influenced by its molecular weight and water solubility.[64,65] Hence, the lower absorption of CHT20 as compared to CHT is explained from the higher molecular weight of grafted copolymer (CHT20) and its reduced solubility in the presence of hydrophobic polyurethane grafting on CHT. However, the results of circulation time clearly indicate that the absorption of the graft copolymer in blood needs 1 h and typical time for excretion/absorption from blood to other organs of the materials takes another 5 h of time totaling 6 h of circulation time in mice.

Distribution of Absorbed Graft Copolymer in Different Organs. The distribution of CHT20 in various organs was checked by measuring the concentration of the polymer in organs at predetermined time after administered the materials orally. The concentrations of CHT20 were investigated in liver, kidney, heart, spleen, lung and thymus of sacrificed mice. It was found that the absorbed CHT/CHT20 molecules were distributed in all the tested organs. The concentration of CHT20 in liver is an important index to reflect the amount of material deposited there. Figure 14b shows the concentration of CHT20 in liver indicating a gradual pile up of material with time. It is obvious that the accumulation of CHT or CHT20 in spleen is higher than it is distributed in other organs (Figure 14,

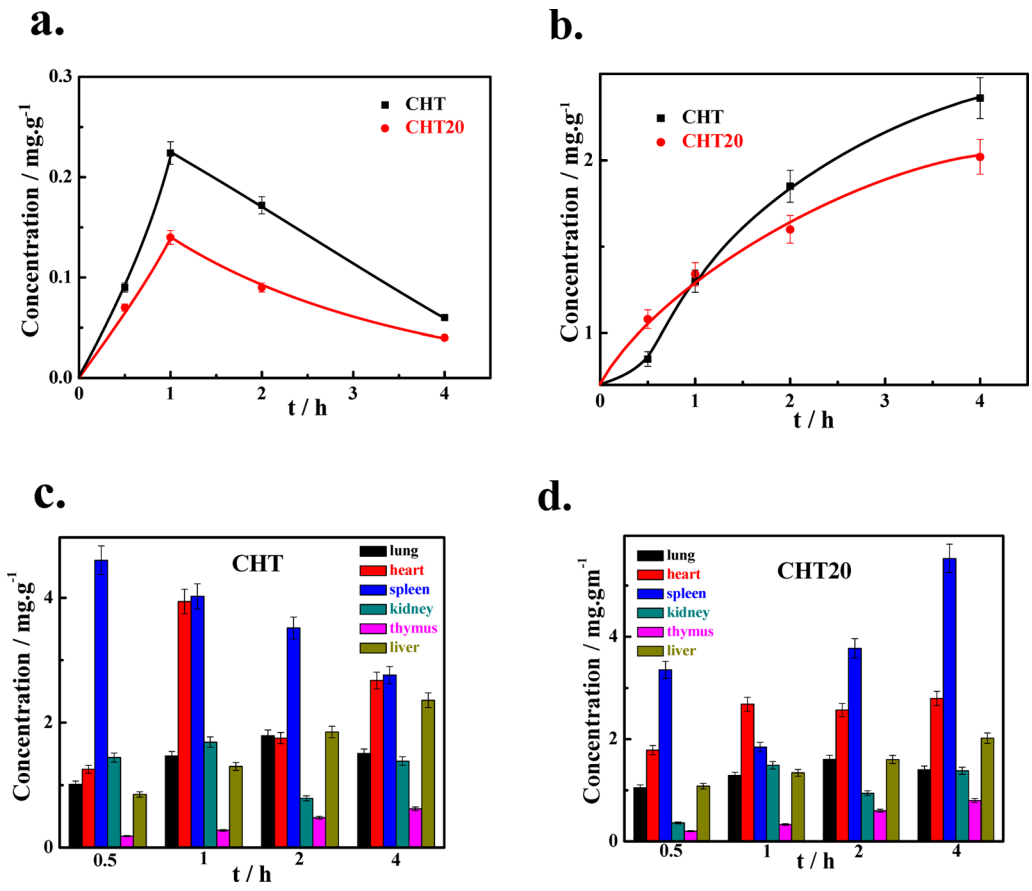

Figure 14. Concentration of CHT and CHT20 as a function of circulation time after oral administration (a) in plasma, and (b) in liver. The concentration of CHT and CHT20 in indicated organs in (c) and (d), respectively, showing relative concentrations in different organs.

DOI: 10.1021/acs.macromol.5b00030
Macromolecules 2015, 48, 2654−2666

parts c and d). However, the accumulation of CHT in various organs is slightly high with respect to CHT20 as explained from the greater absorption of CHT as compared to CHT20 in blood as observed in Figure 14a. In order to understand the effect of accumulated material in different organs, histopathological examinations of major organs including kidney, liver and spleen were conducted (Figure 15). Interestingly, there is no

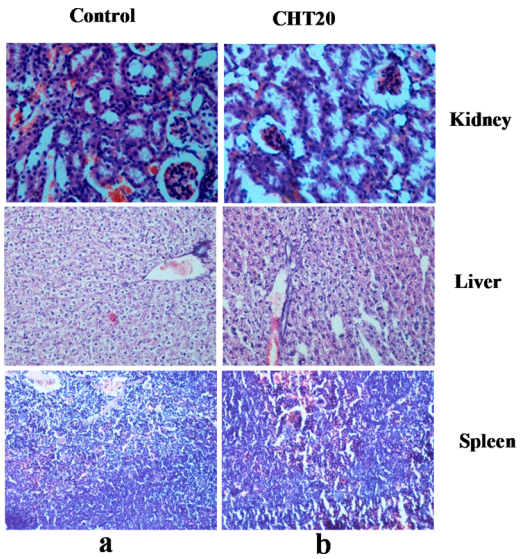

Figure 15. Histopathology of kidney, liver, and spleen tissues fed with (a) PBS and (b) CHT20 after 4 h.

alteration of cell morphology of the organ cells of mice fed with CHT20 as compared to the organs of the mice fed with saline (control). The details of accumulated CHT/CHT20 in different organs as a function of time have been presented in Supporting Information, table S3. The bioavailability of CHT20 along with histopathological testing clearly indicates that graft copolymer is nicely Adsorbed by the body and they do not exhibit any toxicity in different organs as mentioned.

Polyurethane grafting on CHT backbone reduces the hydrophilicity of chitosan while the flexibility increases in graft copolymer. The lowering of hydrophilicity is due to the wrapping up of hydrophobic PU constituent over CHT molecules. Intramolecular hydrogen bonding between CHT molecules makes the system quite rigid but the grafting through PU convert them into relatively flexible system arising from the loss of hydrogen bonding together with addition of soft segment part of PU which provides the extra flexibility. The above phenomena explain the lower elastic modulus and lower glass transition temperature of graft copolymers vis-à-vis CHT. Pure CHT being hydrophilic exhibit large swelling which is manifested in its fast release of drug. On the other hand, network structure in graft copolymer organizes the swelling behavior and thereby controls the drug release in a sustained manner. The biocompatibility including hemocompatibility has increased in graft copolymer significantly raising the use of graft copolymer of chitosan as better biomaterials. The developed novel materials are tested as biomaterials for future work.

CONCLUSION

Chemical modification of chitosan has been performed through grafting with isocyante terminated polyurethane and the degree of substitution has been varied until cross-linking between CHT molecules having a polyurethane bridge. Degree of substitution has been calculated from the deconvoluted peak areas obtained from solid state NMR studies. Spin−lattice relaxation time (T_1) increases with DS due to the relaxation constraints arising from the grafted part on CHT molecules. The extent of solubility and swelling characteristics decreases considerably with increasing DS in graft copolymers as compared to pristine CHT. Simultaneously, hydrophobic character, measured through contact angle, increases due to polyurethane grafting. Significant improvement of toughness has been observed after grafting vis-à-vis pure CHT while cross-linked copolymer exhibit brittle nature under uniaxial elongation. On the contrary, glass transition temperature decrease slightly, as observed in DMA measurement, in graft copolymer revealing flexible nature even after grafting and thereby, make the graft copolymer suitable for applications in biomedical arena. Graft copolymers exhibit sustained release of drug and, thereby, overcome the burst release observed in pure CHT. Chitosan graft copolymers are found to be bio- and hemocompatible in nature as observed through platelet aggregation, cell viability, cell adhesion, and hemolysis studies. Further, graft copolymers do not supply any reactive oxygen in the cell culture and the materials do not affect the biology of circulating blood cells. Therefore, newly developed polyurethane graft chitosans are very much appropriate for controlled drug delivery.

ASSOCIATED CONTENT

Supporting Information

Schematic diagram of obtained grafting product of chitosan modified by polyurethane showing different locations of grafting, figures showing standard curve of CHT and CHT20, graphical representation of spin−lattice relaxation time, complete FTIR spectra of CHT and PU grafted CHT, contact angle of CHT and its graft copolymers, and different mathematical models for drug release mechanism, and tables of release rate constant (k), correlation coefficient (r_2), and diffusion release exponent (n) and percent hemolysis of RBCs. This material is available free of charge via the Internet at http://pubs.acs.org.

AUTHOR INFORMATION

Corresponding Author

*(P.M.) E-mail: pmaiti.mst@itbhu.ac.in.

Notes

The authors declare no competing financial interest.

ACKNOWLEDGMENTS

The authors acknowledge the receipt of funding for his fellowship from *CSIR*, New Delhi, India. The authors also acknowledge the kind support of Prof. N. Misra, School of Biomedical Engineering, IIT (BHU), Varanasi, for UV−vis and contact angle measurements. The authors also acknowledge the receipt of research funding from the Council for Scientific and Industrial Research (CSIR), New Delhi, Government of India (Project No. 02(0074)/12/EMR-II).

REFERENCES

(1) Onishi, H.; Machida, Y. Biodegradation and distribution of water-soluble Chitosan in mice. *Biomaterials* **1999**, *20*, 175−182.

(2) Ravi Kumar, M. N. V.; Muzzarelli, R. A. A.; Muzzareli, C.; Sasfiwa, H.; Domb, A. J. Chitosan Chemistry and Pharmaceutical Perspectives. *Chem. Rev.* **2004**, *104*, 6017−6084.

DOI: 10.1021/acs.macromol.5b00030
Macromolecules 2015, 48, 2654−2666

(3) Muzzarelli, R. A. A.; Muzzarelli, C. Chitosan Chemistry: Relevance to the Biomedical Science. *Adv. Polym. Sci.* **2005**, *186*, 151−209.
(4) Rinaudo, M. Chitin and Chitosan: Properties and applications. *Prog. Polym. Sci.* **2006**, *31*, 603−632.
(5) Ifuku, S.; Morooka, S.; Morimoto, M.; Saimoto, H. Acetylation of chitin Nanofibers and their Transparent Nanocomposite Films. *Biomacromolecules* **2010**, *11*, 1326−1330.
(6) Gong, X.; Peng, S.; Wen, W.; Sheng, P.; Li, W. Design and Fabrication of Magnetically Functionalized core/shell Microspheres for Smart Drug Delivery. *Adv. Funct. Mater.* **2009**, *19*, 292−297.
(7) Hsieha, W. C.; Changb, C. P.; Gaoc, Y. L. Controlled release properties of Chitosan encapsulated volatile Citronella Oil microcapsules by thermal treatments. *Colloids Surf., B* **2006**, *53*, 209−214.
(8) Yamamoto, H.; Amaike, M. Biodegradation of cross-linked chitosan gels by microorganisms. *Macromolecules* **1997**, *30*, 3936−3937.
(9) Risbud, M. V.; Bhonde, R. R. Polyacrylamide-chitosan hydrogels: in vitro biocompatibility and sustained antibiotic release studies. *Drug Deliv* **2000**, *7*, 69−75.
(10) Smitha, B.; Sridhar, S.; Khan, A. A. Chitosan-poly (vinyl pyrrilidine) blends as membranes for direct methanol fuel cell applications. *J. Power Sources* **2006**, *159*, 846−854.
(11) Lubben, I. M. V.; Verhoef, J. C.; Aelst, A. C. V.; Borchard, G.; Junginger, H. E. Chitosan micropartiloces for oral vaccination: preparation, characterization and preliminary in vivo uptake studies in murine Peyer's patches. *Biomaterials* **2001**, *22*, 687−694.
(12) Berthold, A.; Cremer, K.; Kreuter, J. Preparation and characterization of chitoan microsphere as drug carrier for prednisolone sodium phosphate as model for anti inflammatory drugs. *J. Controlled Release* **1996**, *39*, 17−25.
(13) Agnihotri, S. A.; Mallikarjuna, N. N.; Aminabhavi, T. M. Recent advances on chitosan-based micro- and nanoparticles in drug delivery. *J. Controlled Release* **2004**, *100*, 5−28.
(14) Trindade, M. C. D.; Lind, M.; Nakashima, Y.; Sun, D.; Goodman, S. B.; Schurman, D. J.; Smith, R. L. Interleukin-10 inhibits polymethylmethacrylate particle induced interleukin-6 and tumor necrosis factore-release by human monocyte/macrophages in vitro. *Biomaterials* **2001**, *22*, 2067−2073.
(15) Jiang, X.; Dai, H.; Leong, K. W.; Goh, S. H.; Mao, H. Q.; Yang, Y. Y. Chitosan-g-PEG/DNA complexes deliver gene to the rat liver via intrabiliary and intraportal infusions. *J. Gene Med.* **2006**, *8*, 477−487.
(16) Chen, M. H.; Hsu, Y. H.; Lin, C. P.; Chen, Y. J.; Young, T. H. Interactions of acinar cells on biomaterials with various surface properties. *J. Biomed. Mater. Res., Part A* **2005**, *74*, 254−62.
(17) Mao, J. S.; Liu, H. F.; Yin, Y. J.; Yao, K. D. The properties of chitosan-gelatin membranes and scaffold modified with hyaluronic acid by different methods. *Biomaterials* **2003**, *24*, 1621−1629.
(18) Lin, S. J.; Jee, S. H.; Hsaio, W. C.; Lee, S. J.; Young, T. H. Formation of melanocyte spheroids on the chitosan-coated surface. *Biomaterials* **2005**, *26*, 1413−22.
(19) Wang, Y. C.; Lin, M. C.; Wang, D. M.; Hsieh, H. J. Fabrication of a novel porous PGA chitosan hybrid matrix for tissue engineering. *Biomaterials* **2003**, *24*, 1047−57.
(20) Gingras, M.; Paradis, I.; Berthod, F. Nerve regeneration in a collagen-chitosan tissue-engineered skin transplanted on nude mice. *Biomaterials* **2003**, *24*, 1653−61.
(21) Du, Y.; Luo, X. L.; Xu, J. J.; Chen, H. Y. A simple method to fabricate a chitosan-gold nanoparticles film and its application in glucose biosensor. *Bioelechtrochemistry* **2007**, *70*, 342−347.
(22) Oliveiraa, J. M.; Rodriguesa, M. T.; Silva, S. S.; Malafayaa, P. B.; Gomesa, M. E.; Viegasac; Diasc, I. R.; Azevedod, J. T.; Manoa, J. F.; Reisa, R. L. Novel hydroxyapatite/chitosan bilayered scaffold for osteochondral tissue-engineering applications: Scaffold design and its performance when seeded with goat bone marrow stromal cells. *Biomaterials* **2006**, *27*, 6123−6137.
(23) Kumar, M. N. V. R. Nano and microparticles as controlled drug delivery devices. *J. Pharm. Pharmaceut. Sci.* **2000**, *3*, 234−258.
(24) Bodnar, M.; Hartmann, J. F.; Borbely, J. Preparation and characterization of chitosan-based nanoparticles. *Biomacromolecules* **2005**, *6*, 2521−2527.
(25) Zhang, C.; Ping, Q.; Zhang, H.; Shen, J. Preparation of *N*-alkyl-*O*-sulfate chitosan derivatives and micellar solution of taxol. *Carbohydr. Polym.* **2003**, *54*, 137−141.
(26) Zhang, C.; Ping, Q.; Zhang, H. Self-assembly and characterization of paclitaxel-loaded *N*-octyl-*O*-sulfate chitosan micellar system. *Colloid Surf., B* **2004**, *39*, 69−75.
(27) Prabaharan, M.; Mano, J. F. Chitosan-based particles as controlled drug delivery systems. *Drug Deliv* **2005**, *12*, 41−57.
(28) Brar, S.; Yadav, A. Investigation of microstructure of glycidyl methacrylate/α-methyl Styrene copolymers by 1D- and 2D- NMR Spectroscopy. *Eur. Polym. J.* **2003**, *39*, 15−19.
(29) Xu, D.; Meng, Z.; Han, M.; Xi, K.; Jia, X.; Yu, X.; Chen, Q. Novel Blood-Compatible Waterborne Polyurethane using Chitosan as an Extender. *J. Appl. Polym. Sci.* **2008**, *109*, 240−246.
(30) Lin, W. C.; Tseng, C. H.; Yang, M. C. In vitro Hemocompatibility Evaluation of a Thermoplastic Polyurethane Membrane with Surface-Immobilized water-soluble Chitosan and Heparin. *Macromol.Biosci.* **2005**, *5*, 1013−1021.
(31) Pasparakis, G.; Bouropoulos, N. Swelling studies and in vitro release of verapamil from calcium alginate and calcium alginate-chitosan beads. *Int. J. Pharm.* **2006**, *323*, 34−42.
(32) Mary, L. A.; Senthilram, T.; Suganya, S.; Nagarajan, L.; Venugopal, J.; Ramakrishna, S.; Giri Dev, V. R. Centrifugal spun ultrafine fibrous web as a potential drug delivery vehicle. *eXPRESS Polym. Lett.* **2013**, *7*, 238−248.
(33) Singh, S. K.; Singh, M. K.; Nayak, M. K.; Kumari, S.; Gracio, J. A.; Dash, D. Size Distribution Analysis and Physical/Fluorescence Characterization of Graphene Oxide Sheets by Flow Cytometry. *Carbon* **2011**, *49*, 684−692.
(34) Mishra, A.; Singh, S. K.; Dash, D.; Aswal, V. K.; Maiti, B.; Misra, M.; Maiti, P. Self-assembled aliphatic chain extended polyurethane nanobiohybrids: Emarging hemocompatible biomaterials for sustained drug delivery. *Acta Biomater* **2014**, *10*, 2133−2146.
(35) Singh, N. K.; Singh, S. K.; Dash, D.; Gonugunta, P.; Misra, M.; Maiti, P. CNT Induced B-Phase in Polylactide: Uniqe Crystallization, Biodegradation, and Biocompatibility. *J.Phys. Chem. C* **2013**, *117*, 10163−10174.
(36) Ishida, M. Yoshinaga. Solid −State 13C NMR Analyses of the Microphase-Separated Structure of Polyurethane Elastomer. *Macromolecules* **1996**, *29*, 8824−8829.
(37) Saito, H.; Tabeta, R. High-Resolution Solid-state ^{13}C NMR Study of Chitosan and Its Salts with Acids: Conformational Characterization of Polymorphs and Helical Structures as Viewed from the Conformation-Dependent ^{13}C chemical Shift. *Macromolecules* **1987**, *20*, 2424−2430.
(38) Kavianinia, I.; Plieger, P. G.; Kandile, N. G.; Harding, D. R. K. Fixed-bed column studies on a modified chitosan hydrogel for detoxification of aqueous solution from copper (II). *Cabohydr. Polym.* **2012**, *90*, 875−886.
(39) Breitmaier, E.; Spohn, K. H.; Berger, S. ^{13}C Spin-Lattice relaxation Times and the Mobility of Organic Molecules in Solution. *Angew.Chem., Int. Ed.* **1975**, *14*, 144−158.
(40) Chen, C.; Tao, S.; Qiu, X.; Ren, X.; Hu, S. Long-alkane-chain modified *N*-phthaloyl chitosan membranes with controlled permeability. *Cabohydr. Polym.* **2013**, *91*, 269−276.
(41) Kolhe, P.; Kannan, R. M. Improvement in Ductility of Chitosan through Blending and Copolymerization with PEG: FTIR Investigation of Molecular Interaction. *Biomacromolecules* **2003**, *4*, 173−180.
(42) Liu, J.; Wen, X.; Lu, J.; Kan, J.; Jin, C. Free radical mediated grafting of chitosan with caffeic and ferulic acids: Structures and antioxidant activity. *Int. J. Biol. Macromol.* **2014**, *65*, 97−106.
(43) Chen, Y.; Zhou, S.; Yang, H.; Wu, L. Structure Properties of Polyurethane/Nanosilica Composite. *J. Appl. Polym. Sci.* **2005**, *95*, 1032−1039.
(44) Bozic, M.; Gorgieva, S.; Kokol, V. Laccase-mediated functionalization of chitosan by caffeic and gallic acids for modulating

DOI: 10.1021/acs.macromol.5b00030
Macromolecules 2015, 48, 2654−2666

antioxidant and antimicrobial properties. *Carbohydr. Polym.* **2012**, *87*, 2388−2398.
(45) Flory, P. J. *Principles of Polymer Chemistry*; Cornell University Press: Ithaca, NY, 1953.
(46) Welsh, E. R.; Schaur, C. L.; Qadri, S. B.; Price, R. R. Chitosan Cross-linked with a Water-Soluble, Blocked Diisocyanate. 1. Solid State. *Biomacromolecules* **2002**, *3*, 1370−1374.
(47) Kyzas, G. Z.; Siafaka, P. I.; Lambropoulou, D. A.; Lazaridis, N. K.; Bikiaris, D. N. Poly (itaconic acid)-Grafted Chitosan Adsorbents with Different Cross-Linking for Pb(II) and Cd(II) Uptake. *Langmuir* **2014**, *30*, 120−131.
(48) Ganguly, K.; Aminabhavi, T. M.; Kulkarni, R. Colon Targeting of 5-Fluorouracil Using Polyethylene Glycol Cross-linked Chitosan Microspheres Enteric Coated With Cellulose Acetate Phthalate. *Ind. Eng. Chem. Res.* **2011**, *50*, 11797−11807.
(49) Wan, Y.; Wu, H.; Yu, A.; Wen, D. Biodegradable Polylactide /Chitosan Blend Membranes. *Biomacromolecules* **2006**, *7*, 1362−1372.
(50) Rinki, K.; Dutta, P. K.; Hunt, A. J.; Clark, J. H.; Macquarrie, D. J. Preparation of Chitosan based Scaffold using Supercritical Carbon Dioxide. *Macromol. Symp.* **2009**, *277*, 36−42.
(51) Riga, A. T.; Pan, W.; Cahoon, J. Thermal Analysis. In *Comprehensive Desk Reference of Polymer Characterization and Analysis*; Brady, R. F., Ed.; Oxford University Press: New York, 2003; p 305.
(52) Mucha, M.; Pawlak, A. Thermal analysis of chitosan and its blends. *Thermochim. Acta* **2005**, *427*, 69−76.
(53) Garrido, I. Q.; Laterza, B.; Archederra, J. M. M.; Rienda, J. M. B. Characteristic Feature of Chitosan/Glycerol Blends Dynamics. *Macromol. Chem. Phys.* **2006**, *207*, 1742−1751.
(54) Garrido, I. Q.; Gonzalez, V. I.; Arechederra, J. M. M.; Rienda, J. M. B. The role played by the interactions of small molecules with chitosan and their transition temperatures. Glass-forming liquids: 1,2,3-Propantriol (glycerol). *Carbohydr. Polym.* **2007**, *68*, 173−186.
(55) Rivero, S.; Garcia, M. A.; Pinotti, A. Heat Treatment to Modify the Structural and Physical Properties of Chitosan-Based Films. *J. Agric. Food Chem.* **2012**, *60*, 492−499.
(56) Singh, S. K.; Singh, M. K.; Nayak, M. K.; Kumari, S.; Shrivastava, S.; Gracio, J. A. Thrombus inducing property of atomically thin graphene oxide sheets. *ACS Nano* **2011**, *5*, 4987−96.
(57) Singh, N. K.; Purkayastha, B. P. D.; Roy, J. K.; Banik, R. M.; Gonugunta, P.; Misra, M.; Maiti, P. Tuned biodegradation using poly (hydroxybutyrate −co-valerate) nanohybrids: Emerging biomaterials for tissue engineering and drug delivery. *J. Mater. Chem.* **2011**, *21*, 15919−15927.
(58) Bihari, P.; Holzer, M.; Praetner, M.; Fent, J.; Lerchenberger, M.; Reichel, C. A.; Rehberg, M.; Lakatos, S.; Krombach, M. Single-walled carbon nanotubes activate platelets and accelerate thrombus formation in the microcirculation. *Toxicology* **2010**, *269*, 148−54.
(59) Semberova, J.; Lacerda, S. H. D. P.; Simakova, O.; Holada, K.; Gelderman, M. P.; Simak, J. Carbon nanotubes activate blood platelets by inducing extracellular ca^{2+} influx sensitive to calcium entry inhibitors. *Nano Lett.* **2009**, *9*, 3312−7.
(60) Jackson, S. P. Arterial thrombosis-insidious, unpredictable and deadly. *Nat. Med.* **2011**, *17*, 1423−36.
(61) Depan, D.; Kumar, A. P.; Singh, R. P. Cell proliferation and controlled drug release studies of nanohybrids based on chitosan-g-lactic acid and montmorillonite. *Acta Biomater* **2009**, *5*, 93−100.
(62) Devasagayam, T. P. A.; Tilak, J. C.; Bollor, K. K.; Sane, K. S.; Ghaskabdi, S. S.; Rele, R. D. Free Radicals and Antioxidants in Human Health: Current Status and future Prospects. *J. Assoc. Physicicans India* **2004**, *52*, 794−804.
(63) Krotz, F.; Sohn, H. Y.; Pohl, U. Reactive Oxygen species: Players in the Platelet Game. *Arterioscler. Thromb. Vasc. Biol.* **2004**, *24*, 1988−1996.
(64) Chae, S. Y.; Jang, M. K.; Nah, J. W. Influence of molecular weight on oral absorption of water soluble chitosans. *J. Controlled Release* **2005**, *102*, 383−394.
(65) Zeng, L.; Qin, C.; Chi, W.; Li, W. Absorption and distribution of chitosan in mice after oral administration. *Carbohydr. Polym.* **2008**, *71*, 435−440.

DOI: 10.1021/acs.macromol.5b00030
Macromolecules 2015, 48, 2654−2666